

Modulation of microsaccades by spatial frequency during object categorization

Matt Craddock^{1,2*}, Frank Oppermann^{1,3*}, Matthias M. Müller¹,
Jasna Martinovic⁴

¹ Institute of Psychology, University of Leipzig, Germany; ² School of Psychology, University of Leeds, UK; ³ Donders Institute for Brain, Cognition and Behaviour, Radboud University Nijmegen, Netherlands; ⁴ School of Psychology, University of Aberdeen, UK

* Matt Craddock and Frank Oppermann have contributed equally to this manuscript as joint first authors

Running Head: Microsaccades and object spatial frequencies

Send correspondence to:

Matthias M. Müller

Institute of Psychology
University of Leipzig
Neumarkt 9-19
04109 Leipzig
Germany

Tel: +49 - 341 - 97 39 54 3

Fax: +49 - 341 - 97 35 96 9

Email: m.mueller@rz.uni-leipzig.de

Abstract

The organization of visual processing into a coarse-to-fine information processing based on the spatial frequency properties of the input forms an important facet of the object recognition process. During visual object categorization tasks, microsaccades occur frequently. One potential functional role of these eye movements is to resolve high spatial frequency information. To assess this hypothesis, we examined the rate, amplitude and speed of microsaccades in an object categorization task in which participants viewed object and non-object images and classified them as showing either natural objects, man-made objects or non-objects. Images were presented unfiltered (broadband; BB) or filtered to contain only low (LSF) or high spatial frequency (HSF) information. This allowed us to examine whether microsaccades were modulated independently by the presence of a high-level feature – the presence of an object – and by low-level stimulus characteristics – spatial frequency. We found a bimodal distribution of saccades based on their amplitude, with a split between smaller and larger microsaccades at 0.4° of visual angle. The rate of larger saccades ($\geq 0.4^\circ$) was higher for objects than non-objects, and higher for objects with high spatial frequency content (HSF and BB objects) than for LSF objects. No effects were observed for smaller microsaccades ($< 0.4^\circ$). This is consistent with a role for larger microsaccades in resolving HSF information for object identification, and previous evidence that more microsaccades are directed towards informative image regions.

Keywords: microsaccades, eye movements, object categorisation, object identification, spatial frequency

1. Introduction

Object recognition is based on a cascade of feedforward and feedback mechanisms through the visual processing hierarchy (e.g. Bar et al., 2006; Hochstein & Ahissar, 2002; VanRullen, 2007). This cascade may follow a coarse-to-fine sequence in which spatial frequency information may be particularly important for coding information at different spatial and temporal scales (e.g. Bullier, 2001; Goffaux et al., 2010; Hegdé, 2008; Kauffmann, Ramanoel, & Peyrin, 2014). Initial, feedforward processing may rely on low spatial frequencies (LSF), which provide information about many features of the visual input in parallel, activating compatible nodes in a recognition network (e.g. Levin, Takarae, Miner, & Keil, 2001). However, the conscious identification of objects likely requires re-entrant processing (feedback mechanisms) with focused attention onto the location of decisive features of potential objects (e.g. Di Lollo, Enns, & Rensink, 2000; Evans & Treisman, 2005; Hochstein & Ahissar, 2002). High spatial frequency (HSF) information may provide more fine-grained details and boundaries necessary for object identification (e.g. Oliva & Schyns, 1997; Oliva & Torralba, 2006). While a single glance may rapidly capture LSFs in a visual scene, resolving HSFs and fine spatial detail may require microsaccades (Ko, Poletti, & Rucci, 2010; McCamy, Otero-Millan, Stasi, Macknik, & Martinez-Conde, 2014; Otero-Millan, Troncoso, Macknik, Serrano-Pedraza, & Martinez-Conde, 2008; Rucci, 2008; Rucci, Iovin, Poletti, & Santini, 2007; Turatto, Valsecchi, Tamè, & Betta, 2007). Microsaccades are small eye movements – typically up to 1° of visual angle – that occur frequently even during fixation (for reviews, see Martinez-Conde, Macknik, Troncoso, & Hubel, 2009; Martinez-Conde, Otero-Millan, & Macknik, 2013; Melloni, Schwiedrzik, Rodriguez, & Singer, 2009; Rolfs, 2009). The present study investigates how the occurrence of microsaccades depends on the spatial frequency and object information of the visual input.

Spatial frequency information at different scales contributes to object categorization in different ways. LSFs may be processed and reach higher-order areas faster than HSFs (Bar et al., 2006). LSFs provide coarse global image features associated with the rough shape and layout of objects, helping to determine, for example, scene category. Scene category can be extracted at the first glance as reflected in differential cerebral activity after 150 ms, even with visual exposures starting from 20 ms (Fabre-Thorpe, Richard, & Thorpe, 1998; Thorpe, Fize, & Marlot, 1996; VanRullen & Thorpe, 2001). This processing occurs without directly attending the target image and might thus rely on the first feedforward sweep of activation (Li, VanRullen, Koch, & Perona, 2002; Rousselet, Fabre-Thorpe, & Thorpe, 2002; Thorpe, Gegenfurtner, Fabre-Thorpe, & Bülthoff, 2001). LSF processing may form a major part of this initial feedforward sweep (Bullier, 2001).

When comparing pictures of objects filtered for spatial frequency content, intact unfiltered pictures as well as pictures containing both LSF and HSF information showed better performance compared with pictures only containing either LSF or HSF information from around 100 ms of exposure duration (Kihara & Takeda, 2010, 2012). Importantly, the categorization of LSF-only objects outperformed the categorization of HSF objects for the exposure durations of up to 250 ms, suggesting a prior for LSF information in early processing in this kind of categorization task (Kihara & Takeda, 2010). The differences did not change when attentional demands were increased, suggesting that the effects are based on the first feedforward processing (Kihara & Takeda, 2012).

However, the information extracted during feedforward processing does not always allow full, accurate identification of scenes and objects within them. For example, Evans and Treisman (2005) asked their participants to identify animal targets embedded in RSVP streams of distractors, with each image presented for 75-100 ms. The participants failed to identify the targets in more than half of the trials, and also often failed to localize the target

correctly, suggesting that further processing is necessary. After the feedforward sweep comes re-entrant, feedback processing, which is likely directed at processing of HSFs. For example, consistent with the expectation that processing of HSF information follows processing of LSF information, coarse-to-fine, LSF-to-HSF image sequences of scenes elicit greater earlier activation in early occipital areas and both frontal and temporal areas compared to fine-to-coarse HSF-to-LSF sequences (Peyrin et al., 2010).

Eye movements in this period may be particularly important. Microsaccades follow a stereotypical pattern of inhibition and subsequent release after the onset of a visual stimulus, dropping significantly before rebounding to a new peak after approximately 200-400 ms (e.g. Engbert & Kliegl, 2003; Turatto et al., 2007). They are affected by a range of cognitive factors such as task difficulty and attention (Engbert, 2006; Engbert & Kliegl, 2003; Siegenthaler et al., 2014), and change neural processing (Bosman, Womelsdorf, Desimone, & Fries, 2009; Dimigen, Valsecchi, Sommer, & Kliegl, 2009; Martinez-Conde, Macknik, & Hubel, 2000, 2002; Troncoso et al., 2015). The amplitudes of saccades in these studies range from less than 1° of visual angle, which are typically defined as microsaccades (Martinez-Conde et al., 2013; Melloni et al., 2009), up to 1.5° or 2.0° (e.g. Engbert & Kliegl, 2003; Martinez-Conde, Macknik, Troncoso, & Dyar, 2006; Turatto et al., 2007; Yuval-Greenberg, Tomer, Keren, Nelken, & Deouell, 2008). Stimulus and fixation target size may also influence microsaccade amplitude ((McCamy, Najafian Jazi, Otero-Millan, Macknik, & Martinez-Conde, 2013; Otero-Millan, Macknik, Langston, & Martinez-Conde, 2013).

With regard to spatial frequency, there is evidence to suggest that HSF may increase the rate of microsaccades. Microsaccades occur at a higher rate during tasks which require high visual acuity (Ko et al., 2010), show directional biases during tasks that involve discrimination of visual detail (Turatto et al., 2007), and occur more frequently during foveation of faces or other salient objects (Otero-Millan et al., 2008). They also occur more

frequently in more informative regions of visual scenes, such as those with high contrast and low spatial correlation (McCamy et al., 2014). Bonneh, Adini, & Polat (2015) tested microsaccade rates in response to passive viewing of transient Gabor patches with varying spatial frequency. They found that microsaccade latency following release from inhibition increased as spatial frequencies went from middle-level (2 cycles per degree) to higher (8 cycles per degree), which may have produced a later, smaller peak in microsaccade rate. However, microsaccade rates in passive viewing tasks may not reflect performance in more directed, active viewing tasks (e.g. McCamy et al., 2014).

Consistent with a role of microsaccades in object recognition, it has been demonstrated that the rebound peak in the saccade rate after the onset of a visual stimulus is modulated by high-level stimulus properties; for example, it is relatively elevated for objects compared to non-object stimuli (Hassler, Barreto, & Gruber, 2011; Keren, Yuval-Greenberg, & Deouell, 2010; Yuval-Greenberg et al., 2008). However, this evidence comes primarily from investigations of the relationship between microsaccades and a broadband peak in induced gamma band oscillations (~30-100 Hz), observed using the scalp-recorded electroencephalogram (EEG). This signal was considered to be a signature of the activation of an object representation and the binding of the activity of disparate populations of neurons, each representing distinct object features, into a single coherent percept (Tallon-Baudry & Bertrand, 1999). Several authors have convincingly demonstrated that an electrical, muscle-generated signal associated with microsaccades – the saccade spike potential (SSP) – underlies this effect (Hassler et al., 2011; Keren et al., 2010; Yuval-Greenberg et al., 2008). Thus, many of the reported modulations of induced gamma-band activity – for example, by object orientation (Martinovic, Gruber, & Müller, 2007, 2008) – were likely attributable to modulations of the underlying saccade rate in the critical window around 200-400 ms. Directly examining the saccade rate in this time window may thus reveal information

regarding object recognition processes and role of eye-movements to resolve spatial frequency information.

In the present study, we use a living/non-living categorization task to probe the role of spatial frequency in object processing by varying the spatial frequency content of objects. We presented objects either as unfiltered, broadband (BB) images, or filtered to contain only LSF or HSF content. We chose spatial frequency ranges that corresponded to previous studies examining the different roles of HSF and LSF in object recognition (e.g. Bar et al., 2006). These ranges also correspond to the spatial frequency tuning curves observed in orbitofrontal and visual cortices (Fintzi & Mahon, 2013). We expected that we would observe the typical peaks in the saccade rate approximately 200-400 ms after stimulus onset. Given that microsaccades may have a role in resolving fine spatial detail, we expected to see higher rates for HSF and BB images than for images with LSF only. Additionally, we presented non-object trials with spatial frequency content matched to that of the object images. We expected that saccade peak rates would be reduced relative to object trials, in line with previous findings from EEG (e.g. Hassler et al., 2011; Yuval-Greenberg et al., 2008), and in free-viewing of blank scenes (Otero-Millan et al., 2013, 2008). Nevertheless, object versus non-object differences should also reveal whether differences in saccade rate are driven by high-level factors in combination with low-level stimulus properties, or low-level stimulus properties alone: spatial frequency differences on non-object trials would imply the latter. To better characterise the saccades, we also examined their latency, amplitude and peak velocity.

2. Method

2.1 Participants

Twelve participants were recruited; all students from the University of Leipzig (ages 20 to 28; mean = 24). 7 were female, 5 male. All participants reported normal vision. Participants

received course credit for their participation. The study was conducted in line with the requirements of the local ethics committee of the University of Leipzig, and written informed consent was taken in accordance with the Code of Ethics of the World Medical Association (Declaration of Helsinki).

2.2 Stimuli and apparatus

We selected a set of 240 greyscale photographs from a commercial image database (Hemera Photo Objects), which comprised 120 photographs depicting natural objects (e.g. animals, fruit) and 120 showing man-made objects (e.g. furniture, tools). Only photographs showing a single object in isolation were selected. HSF and LSF versions of each object were produced from the unfiltered, broadband images (BB) by multiplying the Fourier energy of the fast Fourier transform of each BB image with a Gaussian filter that either attenuated spatial frequencies below ~ 4.7 cycles per degree (cpd) for HSF images or above ~ 0.9 cpd for LSF images. These settings were comparable to the filtering used by Bar et al. (2006), and also reflect the sensitivities of the visual and orbitofrontal cortices (Fintzi & Mahon, 2013). For each BB, HSF, and LSF image, a matching non-object was created by producing a noise texture with the same amplitude spectrum and spatial frequency content as the original image. This was achieved by randomising the phase of the object image's Fourier transformation. The mean (global luminance) and standard deviation (RMS contrast) of every BB, HSF, and LSF image was adjusted to match the mean global luminance and RMS contrast of the full set of BB images (see Figure 1).

Visual stimuli were presented centrally on a 19-in Eizo FlexScan S1910 monitor at a screen resolution of 1280×1024 pixels, and seen from a viewing distance of 80 cm. Stimulus size (including a grey background) was 400×400 pixels. The stimuli subtended approximately 10 degrees of visual angle in each direction.

Eye movements were recorded at 500 Hz using the EyeLink II (SR Research Ltd., ON, CA). Motions of the participant's head were restrained by using a head rest. Stimulus presentation and data recordings were controlled by the SR Research Experiment Builder software.

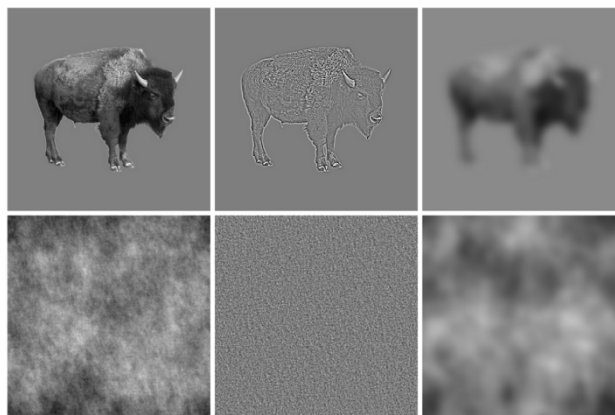


Figure 1 Sample stimuli. Columns show unfiltered, high-pass filtered, and low-pass filtered images. Noise images in the lower row were created by randomising the phase of the FFT of the intact object. All pictures were matched for global luminance and RMS contrast.

2.3 Design

The experiment comprised a two factor design with six different conditions: object (object or non-object noise texture) \times spatial frequency (BB, HSF, LSF). There were 480 trials split across six blocks of 80 trials. The order of trials was randomised for each participant. On half of the trials, participants saw a BB, HSF, or LSF object. Half of these objects were natural, half man-made. On the other half of trials, participants saw a BB, HSF, or LSF non-object texture. The objects presented in each condition were counterbalanced across participants. Thus, each participant saw each object in only one spatial frequency condition, but each object was presented an equal number of times in every condition over the course of the experiment.

Each trial began with a white fixation cross on a black background presented for a variable period of 500-800 ms. A stimulus image was then presented for 500 ms. Then, the fixation cross reappeared and remained on screen for 1000 ms, after which the screen was blanked for a variable period of 900-1200 ms. Participants were encouraged to use this time to blink if they needed to do so. Participants pressed a different button to indicate the category to which each image belonged: natural object, man-made object, or non-object texture. Note that we subsequently collapsed responses across man-made and natural objects, since our primary interest was in the contrast between objects and non-objects. Participants first performed a practice block of 54 trials, which presented a set of practice images created in the same manner as the experimental images but were not shown during the main experiment. Participants were asked to minimize blinking and eye movements while a stimulus or fixation cross was displayed, and to respond as quickly as possible while aiming to minimize errors.

2.4 Behavioural data analysis

Only RTs on correct trials were included in the analysis (3.7% of the data were coded as errors). RTs were considered as outliers and excluded from the analysis when they deviated more than 2.5 standard deviations from the subject's mean in a respective condition (further 1.7% of the data). Reaction times (RTs) and errors were then analysed using a two-way repeated-measures analysis of variance (ANOVA) with the factors Object (Object versus Non-object) and Frequency (BB, HSF, or LSF). Generalized eta squared is reported to estimate the effect size. If required, post-hoc t-tests were conducted with Bonferroni-Holm correction for multiple comparisons.

2.5 Eye-tracking analysis

A time window from 500 ms before to 700 ms after picture onset was selected for analysis. Trials were discarded from the analyses if either (a) a blink was within the analyzed time window, or (b) position data from either of the eyes were missed in the relevant time window. We excluded 4.4% of the data from the analysis. Microsaccades were detected using the Engbert and Mergenthaler procedure (2006; see also Engbert & Kliegl, 2003). This algorithm is based on eye movement velocity, with horizontal and vertical velocities computed separately. The detection threshold was calculated relative to noise as $\lambda = 6$ multiples of the median-based SD. Saccades were determined for each eye separately, but only binocular events with a minimal temporal overlap of 6 ms were accepted. To control for overshoot components, which can result from corrections of fixations after saccades, only saccades which occurred at least 30 ms after the previous saccade were considered as microsaccades (see also Mergenthaler & Engbert, 2010). The saccade rate reflects the estimated number of saccades in a trial per second. The saccade rate was determined in bins of 20 ms. Data were analysed using the same two-way repeated-measures ANOVA as the behavioural data consisting of the factors Object and Frequency.

3. Results

3.1 Behavioural data

Participants responded slower [$F(1, 11) = 61.98, p < .001, \eta_g^2 = .28$] and made more errors [$F(1,11) = 6.00, p = .03, \eta_g^2 = .11$] when responding on object (732 ms; 6.9% errors) than non-object trials (580 ms; 0.4%).

There were significant main effects of Frequency for RTs [$F(2, 22) = 43.76, p < .001, \eta_g^2 = .03$] and errors [$F(2,22) = 5.78, p < .01, \eta_g^2 = .12$] with comparable reaction times and error rates to BB (642 ms, 1.3 % errors) and HSF images (637 ms; 1.1%), and slower and less accurate responses to LSF images (688 ms; 8.6%).

Most important, the interaction between Object and Frequency was also significant for RTs [$F(2, 22) = 21.19, p < .001, \eta_g^2 = .02$] and errors [$F(2,22) = 5.32, p = .01, \eta_g^2 = .11$]. Post-hoc tests (p-value adjusted) revealed that RTs on objects were significantly slower than on non-objects (BB, HSF, and LSF; all $ps < .001$). Additionally, responses to LSF objects (RT: $M = 784$ ms, $SE = 8$ ms; error: $M = 16.7\%$, $SE = 23.5\%$) were slower and more error-prone than responses to both BB (RT: $M = 701$ ms, $SE = 10$ ms, $t(11) = 6.48, p < .001$; error: $M = 2.2\%$, $SE = 2.8\%$, $t(11) = 2.31, p < .05$) and HSF objects (RT: $M = 711$ ms, $SE = 9$ ms, $t(11) = 7.56, p < .001$; error: $M = 1.9\%$, $SE = 2.7\%$, $t(11) = 2.42, p < .05$), while no difference was observed between BB and HSF objects (RT: $t(11) = 1.41, p = .37$; errors: $t < 1$). Furthermore, responses on HSF non-objects (RT: $M = 564$ ms, $SE = 12$ ms) were faster than responses on BB (RT: $M = 583$ ms, $SE = 13$ ms; $t(11) = 4.59, p < .01$) and LSF non-objects (RT: $M = 592$ ms, $SE = 12$ ms; $t(11) = 4.35, p < .01$), while no difference was observed between BB and LSF non-objects ($t(11) = 1.34, p = .37$). There were no differences in error rates between non-object trials (BB: $M = 0.4\%$, $SE = 0.6\%$, HSF: $M = 0.3\%$, $SE = 0.6\%$, LSF: $M = 0.5\%$, $SE = 0.8\%$; $ts < 1$).

3.2 Eye movement data

To determine whether overall saccade rate changes after stimulus presentation, we compared saccade rates averaged across all conditions in three time-windows (baseline: -200-0 ms, poststimulus I: 0-200 ms, and poststimulus II: 200-400 ms). Figure 2 shows the microsaccade rate for each condition averaged across participants. Note that saccade rate is increased before the baseline window. These saccades are likely to reflect movements to re-fixate the fixation cross, which appeared 500 to 800 ms before stimulus onset following a blank screen during which participants was allowed to blink. The saccade rate (baseline: $M = 1.43$ saccades/s; $SE = .19$) decreased after stimulus presentation (poststimulus I: $M = .43$ saccades/s; $SE = .10$; $t-$

test: $t(11) = 9.26, p < .001$) before increasing relative to the baseline in the later time window (poststimulus II: $M = 2.28$ saccades/s; $SE = .26$; t -test: $t(11) = 5.11, p < .001$).

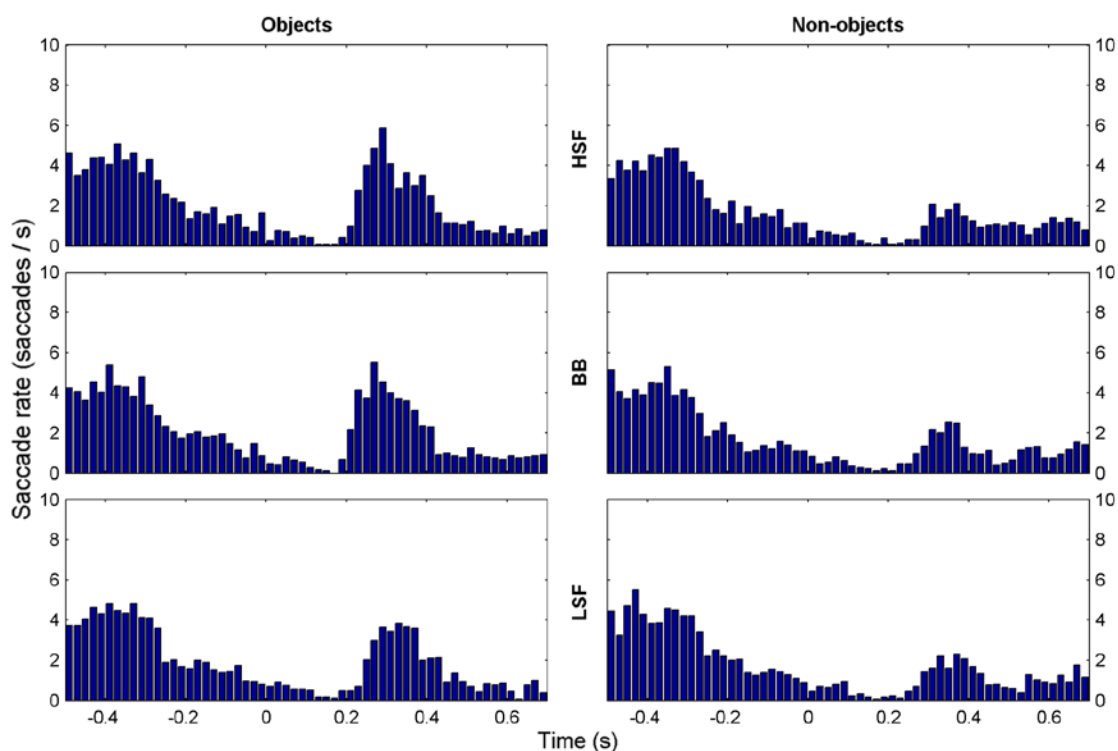


Figure 2 Group ($N = 12$) mean rate of detected eye movements in the eye-tracking experiment over time (bin width = 20 ms), separated by condition. Left column shows eye movements on trials in which objects were present; right column shows movements on trials in which non-objects were presented. From top to bottom, the rows show events when high spatial frequency (HSF), broadband (BB), and low spatial frequency (LSF) images were presented. Note the higher rate of microsaccades in the object conditions from 200-400 ms.

Before comparing saccade rates between conditions, we examined saccade amplitudes. Figure 3 shows the distribution of amplitudes over time averaged across all conditions, with shades of gray reflecting the saccade rate. Overall, saccade amplitudes were mostly between 0.05° and 3° of visual angle. The smallest saccade that we detected with the procedure was 0.03° , which reflects the technical limit of the video-based eye-tracker to measure saccades.

The initial drop in saccade rate after stimulus presentation is clearly visible, with a subsequent increase around 200-400 ms after stimulus presentation. However, as the saccade rate changed over time, the distribution of saccades of different amplitudes also changed. Most interestingly, the saccades in the 200-400 ms time window follow a bimodal amplitude distribution. Smaller saccades peak at a mean amplitude of 0.12° , whereas larger saccades peak around 1.36° . To rule out that this bimodal distribution is driven by a couple of subjects only, we looked at plots of individual subject data (see Supplementary Figure 1). A clear bimodality can be observed for the majority of subjects. Figure 3 also suggests that there may be a latency difference between larger ($M=317\text{ms}$, $SD=24\text{ms}$) and smaller saccades ($M=328\text{ms}$, $SD=35\text{ms}$), but this is not significant ($t(11)<1$, $p=.39$).

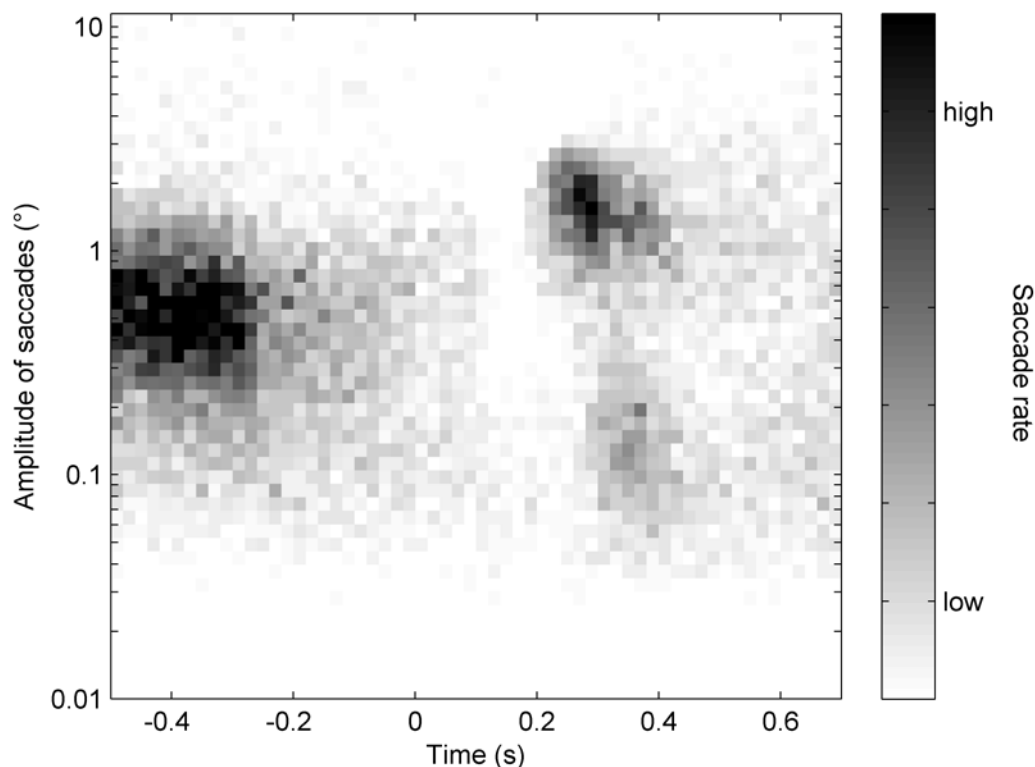


Figure 3 Distribution of saccade amplitudes over time (pooled across subjects ($N = 12$) and conditions; bins of 20 ms and a log amplitude of 0.06). Amplitude axis is plotted on a logarithmic scale. Note the presence of a bimodal distribution after the initial

inhibitory decrease in rate compared to the unimodal distribution in the pre-stimulus window

For further analyses, we focused on the critical time window from 200-400 ms after stimulus onset. Figure 4 shows the clear bimodal distribution of saccade amplitudes in this time window for each condition. While the distribution of the microsaccades seems to be comparable between conditions, the saccade rate differs clearly between conditions for larger saccades. The rate of the larger saccades is higher when objects (bluish bars) rather than non-objects (reddish bars) were presented. We analyzed the saccades around these two distinct peaks of amplitudes separately. The trough between the peaks was used as the boundary with saccades smaller than 0.4° as small microsaccades and saccades larger or equal to 0.4° as large microsaccades (see also Mergenthaler & Engbert, 2010). There are single saccades with amplitudes clearly outside of the two distributions. These outliers were excluded from further analyses of the two saccade types. Saccades were considered as outliers when their amplitude deviated from the participant's mean of the respective conditions more than 2.5 standard deviations. According to this criterion, 4 saccades (0.5 %) were excluded from the analysis of small microsaccades and 24 (1.4 %) from the analysis of large microsaccades. Small microsaccades considered for analysis showed a mean amplitude of 0.12° of visual angle ($SD = 1.32^\circ$). Large microsaccades showed a mean amplitude of 1.27° of visual angle ($SD = 1.30^\circ$).

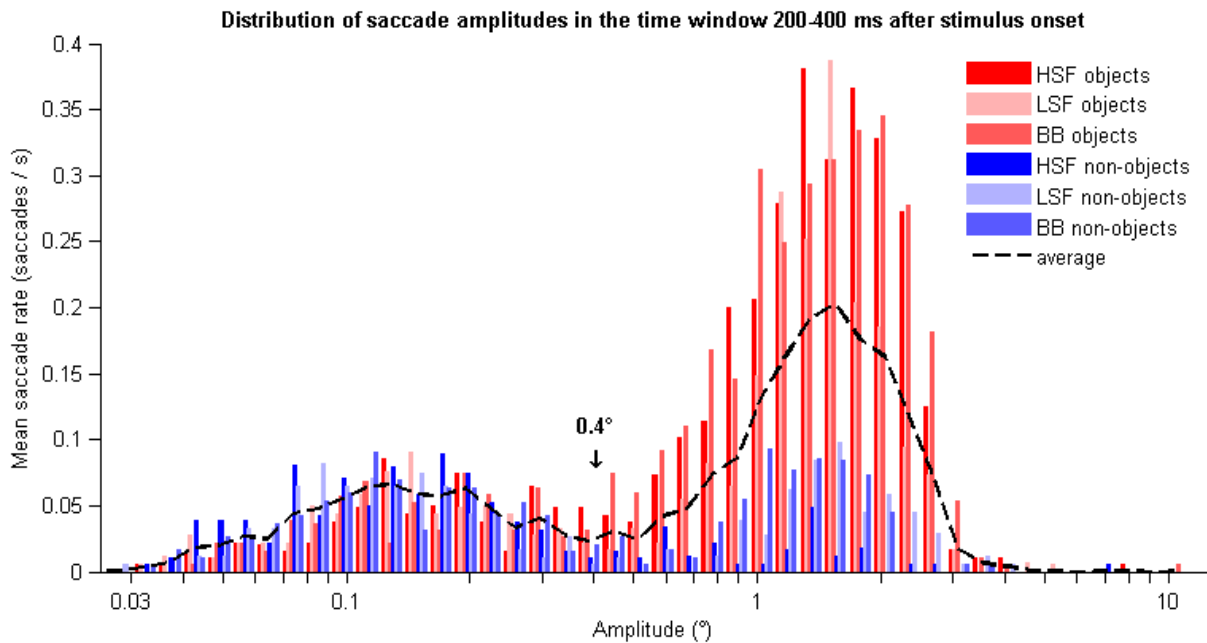


Figure 4 Distribution of saccade amplitudes in the time window from 200-400 ms after stimulus onset averaged across subjects ($N = 12$; bins with a log amplitude of 0.06).

This graph shows the bimodal lognormal distribution of saccade amplitudes in the relevant time window (amplitudes are on a logarithmic scale). The reddish bars reflect the object conditions, the blueish bars the non-object conditions. The black line shows the average across conditions and, thus, reflects the time window 200-400 ms from Figure 3

We analyzed saccade rates, saccade amplitudes, saccade latencies and peak velocity of saccades in the time window 200-400 ms after stimulus onset (Figure 5) using repeated measures ANOVA with the factors Object and Spatial Frequency. In the analysis of amplitudes and peak velocity, subjects were excluded when they made no saccades in one of the conditions in the relevant time window. Thus, three subjects were excluded from the analysis of small microsaccades and five subjects in the analysis of large microsaccades. In the analysis of saccade rate, all subjects were included. 95% confidence intervals for the plots in Figure 5 were estimated using bootstrapping to generate surrogate distributions (1000

iterations) of mean saccade rate, amplitude, and velocity for each condition, as implemented in the ggplot2 package (Wickham, 2009) for R (R Core Team, 2015).

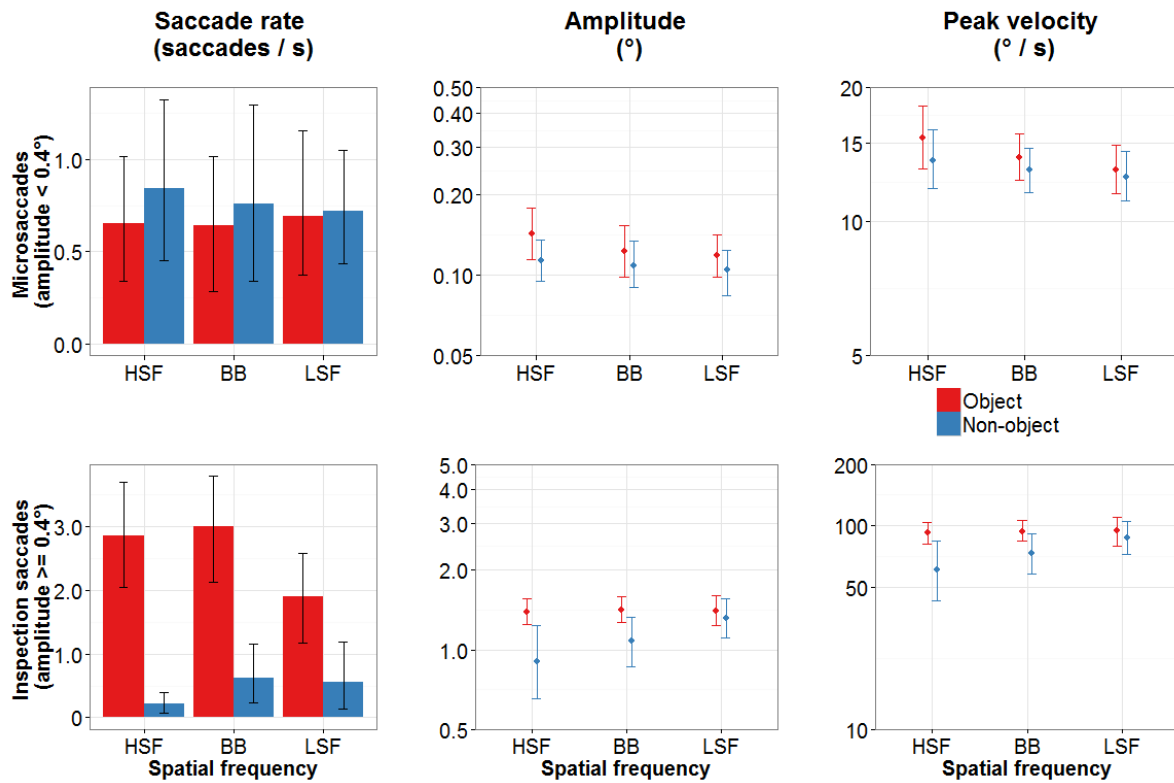


Figure 5 Saccade characteristics separated for the two saccade types in the window from 200-400 ms after stimulus onset for objects (red) and non-objects (blue). The upper row shows microsaccades smaller than 0.4°, the lower row microsaccades of 0.4° and larger. The columns represent different saccade characteristics. Left column shows the saccade rate (N = 12; both rows), the centre column amplitudes (N = 9 upper row, N = 7 lower row), and right column peak velocity (N = 9 upper row, N = 7 lower row). Amplitude and peak velocity are plotted on a log scale. Error bars show bootstrapped 95% confidence intervals, as described in the method. HSF - high spatial frequency, BB - broadband, and LSF - low spatial frequency images

3.2.1 Small microsaccades (amplitude < 0.4°). The analysis of saccade rates revealed no significant effects or interactions [Object: $F(1, 11) = 3.92, p = .07, \eta_g^2 = .01$; Frequency: $F(2, 22) < 1$; Object x Frequency: $F(2, 22) < 1$]. The same was true also for amplitudes [Object: $F(1, 8) = 4.69, p = .06, \eta_g^2 = .07$; Frequency: $F(2, 16) = 1.62, p = .23, \eta_g^2 = .02$; Object x Frequency: $F(2, 16) = 1.36, p = .28, \eta_g^2 = .02$] and latencies (Object: $F(1,9) = 0.10, p=0.75, \eta_g^2 = .002$; Frequency: $F(2,18) = 0.14, p = .87, \eta_g^2 = .004$; Object x Frequency: $F(2,18) = 0.86, p = 0.44, \eta_g^2 = 0.02$). The analysis of peak velocity showed a significant effect of Object, with significantly faster saccades in response to objects than to non-objects [$F(1, 8) = 6.99, p < .05, \eta_g^2 = .06$]. However, no other effects reached significance [Frequency: $F(2, 16) = 3.41, p = .06, \eta_g^2 = .05$; Object x Frequency: $F(2, 16) = 2.02, p = .17, \eta_g^2 = .01$].

3.2.2 Large microsaccades (amplitude $\geq 0.4^\circ$). The analysis of saccade rate revealed significant main effects of Object [$F(1, 11) = 37.53, p < .001, \eta_g^2 = .46$] and of Frequency [$F(2, 22) = 12.44, p < .001, \eta_g^2 = .04$] as well as a significant interaction of Object and Frequency [$F(2, 22) = 16.54, p < .001, \eta_g^2 = .05$]. Subsequent t-tests (p-value adjusted) revealed for all Frequency conditions higher saccade rates for objects compared with non-objects [BB: $t(11) = 6.28, p < .001$; HSF: $t(11) = 6.09, p < .001$; LSF: $t(11) = 4.58, p < .01$]. While the different non-object conditions did not differ [BB vs. HSF: $t(11) = 1.98, p > .29$ BB vs. LSF: $t(11) < 1$; HSF vs. LSF: $t(11) = 1.45, p = .53$], we found differences between object conditions. The saccade rate for HSF objects as well as for BB objects was higher compared with LSF objects [HSF vs. LSF: $t(11) = 6.61, p < .001$; BB vs. LSF: $t(11) = 7.18, p < .001$], whereas HSF objects and BB objects did not differ [$t(11) = 1.38, p = .53$].

Overall, the number of large microsaccades to non-objects was very low. Five out of the 12 participants did not show any saccade in one of the spatial frequency conditions. Therefore, we refrain from analyzing amplitudes, latencies and peak velocity for non-object conditions. For the analysis of object conditions, we found no significant effects of

Frequency in the analyses of amplitudes and peak velocity [$F_s < 1$]. However, we do find a significant effect of Frequency in the analysis of latencies ($F(2,22) = 21.46, p < 0.001, \eta_g^2 = .31$). Subsequent t-tests (p-value adjusted) reveal that latencies from all three conditions are significantly different from each other, with BB objects eliciting the fastest saccades ($M = 292\text{ms}, SD=21\text{ms}$), followed by HSF objects ($M=312\text{ms}, SD=29\text{ms}$), with slowest saccades for LSF objects ($M=335\text{ms}, SD=29\text{ms}$; BB vs. HSF: $t(11)=4.13, p = .003$; BB vs. LSF: $t(11)=5.81, p<.001$; HSF vs. LSF: $t(11)=3.18, p=.009$).

4. Discussion

We investigated modulations of microsaccades during an object categorization task in which objects or non-objects were presented with different scales of spatial frequency content. The images were either unfiltered, broadband images, or filtered to contain only HSF or LSF information. This allowed us to examine both high-level factors (i.e. the presence or absence of an object) and low-level factors (i.e. spatial frequency content) simultaneously. We observed the typical decrease and subsequent increase in saccade rate after visual stimulus presentation (e.g., Engbert & Kliegl, 2003). Most relevant in the context of our study was the clear peak in saccade rate in the time window 200 to 400 ms after stimulus onset. The size and presence of this peak was modulated by the experimental manipulations. Specifically, the peak rate was higher on object than non-object trials, as predicted on the basis of previous work, and was higher for HSF and BB objects than for LSF objects.

Detailed analysis of the eye-tracking data revealed a bimodal distribution of the amplitudes of saccades in response to the stimuli, suggesting two different classes of saccade: small microsaccades with amplitudes below 0.4° , and large microsaccades with amplitudes above 0.4° (Mergenthaler & Engbert, 2010). While it is tempting to suggest that small and large microsaccades are generated by different underlying mechanisms, Otero-Millan et al.

(2013) argued that microsaccades and saccades fall on the same functional continuum, and found that saccade rates across that continuum increase as stimulus size increases. Otero-Millan et al. used a free-viewing paradigm in which all saccades over a 30-s trial are considered. These saccades showed a unimodal amplitude distribution with a peak depending on the stimulus size. In contrast, our results reflect the initial burst of saccades 200-400 ms after stimulus onset during a brief stimulus presentation of 500 ms. Small microsaccades in our study show the same characteristics (amplitude and peak velocity) as observed for fixational events in Otero-Millan et al.'s study; our participants were asked to fixate a fixation cross before and after stimulus exposure. Large microsaccades in our study show similar amplitude and peak velocity as those in response to objects of comparable visual size (~4 to 8°). Thus, the bimodal distribution we observe may reflect the sum of trials in which the eyes remain fixated and trials in which the stimuli are inspected during this time window, and thus may reflect both the demands of the task and the size of our stimuli, rather than different classes of eye movement.

Otero-Millan et al. (2011) also found that microsaccades larger than 0.5° tended to generate a corrective microsaccade, resulting in a square wave jerk. Corrective saccades may be particularly likely with our object stimuli, given that participants are required to discriminate between different categories, and must therefore inspect informative image regions closely. Nevertheless, we found that our experimental manipulations had very little effect on small microsaccades: there were no substantial effects of object or of spatial frequency observed in the microsaccade rate, amplitude, or peak velocity. In contrast, the large microsaccades were significantly affected by both the presence of an object and by the spatial frequency content of the stimulus. Specifically, for large microsaccades, there were higher saccade rates for objects than for non-objects. Furthermore, there were higher saccade rates for HSF and BB objects than for LSF objects. For non-objects, there were no

differences in rate across different spatial frequencies. This suggests that when objects are presented, more goal-directed inspection saccades may have been necessary to resolve the spatial frequency information supporting object recognition. LSF objects also elicited slower microsaccades than BB or HSF objects, but BB objects elicited even faster microsaccades than HSF objects, indicating the importance of joining low and high spatial frequency information for efficient guidance of eye movements. We suggest that this is consistent with a first-pass, feedforward sweep determining if and where closer inspection was necessary, with feedback mechanisms guiding small eye movements in resolving fine spatial detail (Ko et al., 2010; Poletti, Listorti, & Rucci, 2013). Our findings are also consistent with McCamy et al.'s (2014) finding that more microsaccades are directed to highly informative image regions.

One additional possibility is that the additional task required for objects – discrimination between living and non-living objects – may in part be responsible for increasing the rate of larger microsaccades. We previously reported an increased rate of microsaccades for objects versus non-objects in a task with a very different set of object and non-object stimuli (Kosilo et al., 2013). No additional task beyond discriminating between objects and non-objects was required in our previous study, suggesting that it is unlikely that the additional task performed on objects here would explain all of the difference in microsaccade rate between objects and non-objects. An account that combines bottom-up, stimulus-driven effects with top-down task requirements is a more likely explanation.

Given the timing of our effects – 200 to 400 ms after stimulus onset – one might ask to what extent these saccades contribute to correct object categorization. Previous studies suggested that reasonably accurate broad categorization of objects is possible even with exposure durations of around 100 ms or less (Thorpe et al., 1996; VanRullen & Thorpe, 2001). However, participants are often not able to identify the target objects correctly beyond

the initial broad categorization (see Evans & Treisman, 2005). These earlier studies often used clear circumscribed categories as animal or vehicle sharing specific features (e.g., most animals have legs) that can be used by the participants to categorize the target object without identification. In addition, these target objects were often embedded in scenes that provided further information on the gist of the scene. Moreover, categorization performance in our task is much higher compared to the previous studies, at least in object conditions containing HSF information (around 2.1% errors in HSF and BB object condition). While previous studies suggested that LSF information is more relevant for object categorization with limited exposure duration (Kihara & Takeda, 2010, 2012), our study clearly demonstrates that HSF information contributes to enhance categorization performance (cf. the error rate of 16.6% in the LSF object condition). The advantage of HSF information was not only found in error rates but also RTs were much faster in the HSF and BB object condition compared with LSF condition. Nevertheless, the categorization responses on objects took more than 700 ms on average, and even the fastest response for a correct object categorization took more than 400 ms. In summary, saccades in this time window might well be supporting object identification in our categorization task.

Note that in a previous report, we found that microsaccades were moderated by high-level and low-level stimulus properties independently (Kosilo et al., 2013). Kosilo et al.'s (2013) experiment required participants to discriminate between line drawings of objects and non-objects that were closely matched to them in terms of various visual attributes, whilst this study used noise texture patches as non-objects. The linear, high-frequency content of non-objects in Kosilo et al. (2013) could have led to more microsaccades in the non-object condition. Also, the specific low-level property which was manipulated differed across studies (spatial frequency here; chromoluminance content there), so it is possible that high-level/low-level interactions depend on the stimulus property which is manipulated.

The bimodal distribution of saccades in the present study has also important methodical implications. When considering that differences between conditions in the present study were only found for large microsaccades but not for small microsaccades, averaging across all saccades can lead to invalid conclusions. Larger saccades are accompanied by larger amplitudes and larger peak velocities. Thus, by averaging across all saccades, the difference in the saccade rate of the inspection saccades would result in differences of the mean amplitude and the mean peak velocity as well. However, these differences do not reflect that larger or faster saccades were produced in a specific condition. Rather, it reflects that overall more of the larger and faster saccades were produced. Some previous studies reporting effects of cognitive factors on microsaccades subsume saccades with amplitudes up to 1.5° or 2.0° (e.g. Engbert & Kliegl, 2003; Turatto et al., 2007; Yuval-Greenberg et al., 2008), although other studies have already considered a detailed analysis of saccade size in relationship to various stimulus properties (e.g. McCamy et al., 2012; Otero-Millan et al., 2008; Troncoso et al., 2015). Given our finding, future research should take a closer look at attributes of saccades elicited in their experiments and if they are found to fall within discrete parts of the saccade continuum, they should be analysed separately. This will help to further determine the functional role of microsaccades.

The findings of our study also bear methodological relevance for researchers wishing to examine the induced gamma band signal using EEG, which is highly susceptible to artefacts related to such eye movements. Although previous examinations of microsaccades in comparable paradigms to those used in EEG have suggested that not all patterns of induced gamma-band activity mirror those found in eye movements (Makin et al., 2011), we would nevertheless suggest caution when the microsaccade rate cannot be directly examined via eye-tracking or detection of miniature eye movements from eye channels (Craddock, Martinovic, & Müller, 2016). A task that requires discrimination of complex stimuli is likely

to lead to large microsaccades even in the presence of the fixation cross (Kosilo et al., 2013). Our study indicates that these eye movements reflect both low-level and high-level properties of the stimulus in a way which is consistent with their role in sustaining efficient recognition by guiding the acquisition of task-relevant information. Thus, any study of induced GBA that does not account for microsaccadic artefact is likely to be confounding a range of bottom-up and top-down effects that may be ocular or neural in origin.

In summary, the implications of our findings are clear: small saccadic eye movements may be influenced by a combination of both high and low-level factors, and thus researchers must be aware of this when manipulating such factors simultaneously. The finding that spatial frequency content of images is differently utilised when categorising objects, as opposed to distinguishing them from noise texture patches, fits well within the tenets of object recognition models that posit a special role for low-level, spatial frequency information content (e.g. Bar et al., 2006; Bullier, 2001; Hegdé, 2008; Sowden & Schyns, 2006). Furthermore, our study demonstrates that depending on the attributes of the stimuli and the task, different manifestations of saccades may be observed. These different types of saccades may come from discrete parts of the saccade continuum - in our study, as in Mergenthaler and Engbert (2010), we observed both small and large (i.e., $> 1^\circ$) microsaccades. Although small microsaccades were not modulated by low or high-level factors, large microsaccades were, shedding further light on the strategic role of eye movements in sampling the visual environment in order to acquire task-relevant information - in this case, fine spatial detail that is indicative of object identity.

Acknowledgements

The project was funded by the Deutsche Forschungsgemeinschaft (DFG, MU 972/16-1). The funders had no role in the design, collection, analysis and interpretation of data, in the writing of the manuscript, or in the decision to submit the manuscript for publication.

References

- Bar, M., Kassam, K. S., Ghuman, A. S., Boshyan, J., Schmid, A. M., Dale, A. M., ... Halgren, E. (2006). Top-down facilitation of visual recognition. *Proceedings of the National Academy of Sciences*, *103*(2), 449–454. <http://doi.org/10.1073/pnas.0507062103>
- Bonneh, Y. S., Adini, Y., & Polat, U. (2015). Contrast sensitivity revealed by microsaccades. *Journal of Vision*, *15*(9), 11–11.
- Bosman, C. A., Womelsdorf, T., Desimone, R., & Fries, P. (2009). A Microsaccadic Rhythm Modulates Gamma-Band Synchronization and Behavior. *The Journal of Neuroscience*, *29*(30), 9471 – 9480. <http://doi.org/10.1523/JNEUROSCI.1193-09.2009>
- Bullier, J. (2001). Integrated model of visual processing. *Brain Research Reviews*, *36*(2-3), 96–107. [http://doi.org/10.1016/S0165-0173\(01\)00085-6](http://doi.org/10.1016/S0165-0173(01)00085-6)
- Craddock, M., Martinovic, J., & Müller, M. M. (2016). Accounting for microsaccadic artifacts in the EEG using independent component analysis and beamforming. *Psychophysiology*, *53*(4), 553–565. <http://doi.org/10.1111/psyp.12593>
- Di Lollo, V., Enns, J. T., & Rensink, R. A. (2000). Competition for consciousness among visual events: The psychophysics of reentrant visual processes. *Journal of Experimental Psychology: General*, *129*(4), 481–507. <http://doi.org/10.1037/0096-3445.129.4.481>
- Dimigen, O., Valsecchi, M., Sommer, W., & Kliegl, R. (2009). Human Microsaccade-Related Visual Brain Responses. *The Journal of Neuroscience*, *29*(39), 12321 –12331. <http://doi.org/10.1523/JNEUROSCI.0911-09.2009>
- Engbert, R. (2006). Microsaccades: a microcosm for research on oculomotor control, attention, and visual perception. In S. L. M. S. Martinez-Conde (Ed.), *Progress in Brain Research* (Vol. Volume 154, Part A, pp. 177–192). Elsevier. Retrieved from <http://www.sciencedirect.com/science/article/pii/S0079612306540099>
- Engbert, R., & Kliegl, R. (2003). Microsaccades uncover the orientation of covert attention. *Vision Research*, *43*(9), 1035–1045. [http://doi.org/10.1016/S0042-6989\(03\)00084-1](http://doi.org/10.1016/S0042-6989(03)00084-1)

- Evans, K. K., & Treisman, A. (2005). Perception of Objects in Natural Scenes: Is It Really Attention Free? *Journal of Experimental Psychology: Human Perception and Performance*, *31*(6), 1476–1492. <http://doi.org/10.1037/0096-1523.31.6.1476>
- Fabre-Thorpe, M., Richard, G., & Thorpe, S. J. (1998). Rapid categorization of natural images by rhesus monkeys. *Neuroreport*, *9*(2), 303–308.
- Fintzi, A. R., & Mahon, B. Z. (2013). A Bimodal Tuning Curve for Spatial Frequency Across Left and Right Human Orbital Frontal Cortex During Object Recognition. *Cerebral Cortex*. <http://doi.org/10.1093/cercor/bhs419>
- Goffaux, V., Peters, J., Haubrechts, J., Schiltz, C., Jansma, B., & Goebel, R. (2010). From Coarse to Fine? Spatial and Temporal Dynamics of Cortical Face Processing. *Cerebral Cortex*. <http://doi.org/10.1093/cercor/bhq112>
- Hassler, U., Barreto, N. T., & Gruber, T. (2011). Induced gamma band responses in human EEG after the control of miniature saccadic artifacts. *NeuroImage*, *57*(54), 1411–1421. <http://doi.org/10.1016/j.neuroimage.2011.05.062>
- Hegd , J. (2008). Time course of visual perception: Coarse-to-fine processing and beyond. *Progress in Neurobiology*, *84*(4), 405–439. <http://doi.org/10.1016/j.pneurobio.2007.09.001>
- Hochstein, S., & Ahissar, M. (2002). View from the Top. *Neuron*, *36*(5), 791–804. [http://doi.org/10.1016/S0896-6273\(02\)01091-7](http://doi.org/10.1016/S0896-6273(02)01091-7)
- Kauffmann, L., Ramanoel, S., & Peyrin, C. (2014). The neural bases of spatial frequency processing during scene perception. *Frontiers in Integrative Neuroscience*, *8*. <http://doi.org/10.3389/fnint.2014.00037>
- Keren, A. S., Yuval-Greenberg, S., & Deouell, L. Y. (2010). Saccadic spike potentials in gamma-band EEG: Characterization, detection and suppression. *NeuroImage*, *49*(3), 2248–2263. <http://doi.org/10.1016/j.neuroimage.2009.10.057>

- Kihara, K., & Takeda, Y. (2010). Time course of the integration of spatial frequency-based information in natural scenes. *Vision Research*, *50*(21), 2158–2162.
<http://doi.org/10.1016/j.visres.2010.08.012>
- Kihara, K., & Takeda, Y. (2012). Attention-free integration of spatial frequency-based information in natural scenes. *Vision Research*, *65*, 38–44. <http://doi.org/10.1016/j.visres.2012.06.008>
- Ko, H., Poletti, M., & Rucci, M. (2010). Microsaccades precisely relocate gaze in a high visual acuity task. *Nature Neuroscience*, *13*(12), 1549–1553. <http://doi.org/10.1038/nn.2663>
- Kosilo, M., Wuerger, S. M., Craddock, M., Jennings, B. J., Hunt, A. R., & Martinovic, J. (2013). Low-level and high-level modulations of fixational saccades and high frequency oscillatory brain activity in a visual object classification task. *Perception Science*, *4*, 948.
<http://doi.org/10.3389/fpsyg.2013.00948>
- Levin, D. T., Takarae, Y., Miner, A. G., & Keil, F. (2001). Efficient visual search by category: Specifying the features that mark the difference between artifacts and animals in preattentive vision. *Perception & Psychophysics*, *63*(4), 676–697. <http://doi.org/10.3758/BF03194429>
- Li, F. F., VanRullen, R., Koch, C., & Perona, P. (2002). Rapid natural scene categorization in the near absence of attention. *Proceedings of the National Academy of Sciences*, *99*(14), 9596–9601.
<http://doi.org/10.1073/pnas.092277599>
- Makin, A. D. J., Ackerley, R., Wild, K., Poliakoff, E., Gowen, E., & El-Deredy, W. (2011). Coherent illusory contours reduce microsaccade frequency. *Neuropsychologia*, *49*(9), 2798–2801.
<http://doi.org/10.1016/j.neuropsychologia.2011.06.001>
- Martinez-Conde, S., Macknik, S. L., & Hubel, D. H. (2000). Microsaccadic eye movements and firing of single cells in the striate cortex of macaque monkeys. *Nature Neuroscience*, *3*(3), 251–258.
<http://doi.org/10.1038/72961>
- Martinez-Conde, S., Macknik, S. L., & Hubel, D. H. (2002). The function of bursts of spikes during visual fixation in the awake primate lateral geniculate nucleus and primary visual cortex.

Proceedings of the National Academy of Sciences, 99(21), 13920–13925.

<http://doi.org/10.1073/pnas.212500599>

Martinez-Conde, S., Macknik, S. L., Troncoso, X. G., & Dyar, T. A. (2006). Microsaccades Counteract

Visual Fading during Fixation. *Neuron*, 49(2), 297–305.

<http://doi.org/10.1016/j.neuron.2005.11.033>

Martinez-Conde, S., Macknik, S. L., Troncoso, X. G., & Hubel, D. H. (2009). Microsaccades: a

neurophysiological analysis. *Trends in Neurosciences*, 32(9), 463–475.

<http://doi.org/16/j.tins.2009.05.006>

Martinez-Conde, S., Otero-Millan, J., & Macknik, S. L. (2013). The impact of microsaccades on vision:

towards a unified theory of saccadic function. *Nature Reviews Neuroscience*, 14(2), 83–96.

<http://doi.org/10.1038/nrn3405>

Martinovic, J., Gruber, T., & Müller, M. M. (2007). Induced Gamma Band Responses Predict

Recognition Delays during Object Identification. *Journal of Cognitive Neuroscience*, 19(6),

921–934. <http://doi.org/10.1162/jocn.2007.19.6.921>

Martinovic, J., Gruber, T., & Müller, M. M. (2008). Coding of Visual Object Features and Feature

Conjunctions in the Human Brain. *PLoS ONE*, 3(11), e3781.

<http://doi.org/10.1371/journal.pone.0003781>

Martinovic, J., Gruber, T., Ohla, K., & Müller, M. M. (2009). Induced Gamma-band Activity Elicited by

Visual Representation of Unattended Objects. *Journal of Cognitive Neuroscience*, 21(1), 42–

57. <http://doi.org/10.1162/jocn.2009.21004>

McCamy, M. B., Najafian Jazi, A., Otero-Millan, J., Macknik, S. L., & Martinez-Conde, S. (2013). The

effects of fixation target size and luminance on microsaccades and square-wave jerks. *PeerJ*,

1, e9. <http://doi.org/10.7717/peerj.9>

McCamy, M. B., Otero-Millan, J., Macknik, S. L., Yang, Y., Troncoso, X. G., Baer, S. M., ... Martinez-

Conde, S. (2012). Microsaccadic Efficacy and Contribution to Foveal and Peripheral Vision.

The Journal of Neuroscience, 32(27), 9194–9204. <http://doi.org/10.1523/JNEUROSCI.0515-12.2012>

McCamy, M. B., Otero-Millan, J., Stasi, L. L. D., Macknik, S. L., & Martinez-Conde, S. (2014). Highly Informative Natural Scene Regions Increase Microsaccade Production during Visual Scanning. *The Journal of Neuroscience*, 34(8), 2956–2966.

<http://doi.org/10.1523/JNEUROSCI.4448-13.2014>

Melloni, L., Schwiedrzik, C. M., Rodriguez, E., & Singer, W. (2009). (Micro)Saccades, corollary activity and cortical oscillations. *Trends in Cognitive Sciences*, 13(6), 239–245.

<http://doi.org/16/j.tics.2009.03.007>

Mergenthaler, K., & Engbert, R. (2010). Microsaccades are different from saccades in scene perception. *Experimental Brain Research*, 203(4), 753–757. <http://doi.org/10.1007/s00221-010-2272-9>

Oliva, A., & Schyns, P. G. (1997). Coarse Blobs or Fine Edges? Evidence That Information Diagnosticity Changes the Perception of Complex Visual Stimuli. *Cognitive Psychology*, 34(1), 72–107.

<http://doi.org/10.1006/cogp.1997.0667>

Oliva, A., & Torralba, A. (2006). Chapter 2 Building the gist of a scene: the role of global image features in recognition. In S. L. M. L. M. Martinez, J. -M. Alonso and P. U. Tse S. Martinez-Conde (Ed.), *Progress in Brain Research* (Vol. 155, Part B, pp. 23–36). Elsevier. Retrieved from <http://www.sciencedirect.com/science/article/pii/S0079612306550022>

Otero-Millan, J., Macknik, S. L., Langston, R. E., & Martinez-Conde, S. (2013). An oculomotor continuum from exploration to fixation. *Proceedings of the National Academy of Sciences*, 110(15), 6175–6180. <http://doi.org/10.1073/pnas.1222715110>

Otero-Millan, J., Serra, A., Leigh, R. J., Troncoso, X. G., Macknik, S. L., & Martinez-Conde, S. (2011). Distinctive Features of Saccadic Intrusions and Microsaccades in Progressive Supranuclear Palsy. *The Journal of Neuroscience*, 31(12), 4379–4387.

<http://doi.org/10.1523/JNEUROSCI.2600-10.2011>

- Otero-Millan, J., Troncoso, X. G., Macknik, S. L., Serrano-Pedraza, I., & Martinez-Conde, S. (2008). Saccades and microsaccades during visual fixation, exploration, and search: Foundations for a common saccadic generator. *Journal of Vision, 8*(14), 21. <http://doi.org/10.1167/8.14.21>
- Peyrin, C., Michel, C. M., Schwartz, S., Thut, G., Seghier, M., Landis, T., ... Vuilleumier, P. (2010). The Neural Substrates and Timing of Top-Down Processes during Coarse-to-Fine Categorization of Visual Scenes: A Combined fMRI and ERP Study. *Journal of Cognitive Neuroscience, 22*(12), 2768–2780. <http://doi.org/10.1162/jocn.2010.21424>
- Poletti, M., Listorti, C., & Rucci, M. (2013). Microscopic Eye Movements Compensate for Nonhomogeneous Vision within the Fovea. *Current Biology, 23*(17), 1691–1695. <http://doi.org/10.1016/j.cub.2013.07.007>
- R Core Team. (2015). *R: A language and environment for statistical computing*. Vienna, Austria: R Foundation for Statistical Computing. Retrieved from <http://www.r-project.org>
- Rolfs, M. (2009). Microsaccades: Small steps on a long way. *Vision Research, 49*(20), 2415–2441. <http://doi.org/10.1016/j.visres.2009.08.010>
- Rousselet, G. A., Fabre-Thorpe, M., & Thorpe, S. J. (2002). Parallel processing in high-level categorization of natural images. *Nature Neuroscience, 5*(7), 629–630. <http://doi.org/10.1038/nn866>
- Rucci, M. (2008). Fixational eye movements, natural image statistics, and fine spatial vision. *Network: Computation in Neural Systems, 19*(4), 253–285. <http://doi.org/10.1080/09548980802520992>
- Rucci, M., Iovin, R., Poletti, M., & Santini, F. (2007). Miniature eye movements enhance fine spatial detail. *Nature, 447*(7146), 852–855. <http://doi.org/10.1038/nature05866>
- Siegenthaler, E., Costela, F. M., McCamy, M. B., Di Stasi, L. L., Otero-Millan, J., Sonderegger, A., ... Martinez-Conde, S. (2014). Task difficulty in mental arithmetic affects microsaccadic rates and magnitudes. *European Journal of Neuroscience, 39*(2), 287–294. <http://doi.org/10.1111/ejn.12395>

- Sowden, P. T., & Schyns, P. G. (2006). Channel surfing in the visual brain. *Trends in Cognitive Sciences*, 10(12), 538–545. <http://doi.org/10.1016/j.tics.2006.10.007>
- Tallon-Baudry, C., & Bertrand, O. (1999). Oscillatory gamma activity in humans and its role in object representation. *Trends in Cognitive Sciences*, 3(4), 151–162. [http://doi.org/10.1016/S1364-6613\(99\)01299-1](http://doi.org/10.1016/S1364-6613(99)01299-1)
- Thorpe, S., Fize, D., & Marlot, C. (1996). Speed of processing in the human visual system. *Nature*, 381(6582), 520–522. <http://doi.org/10.1038/381520a0>
- Thorpe, S., Gegenfurtner, K. R., Fabre-Thorpe, M., & Bülthoff, H. H. (2001). Detection of animals in natural images using far peripheral vision. *European Journal of Neuroscience*, 14(5), 869–876. <http://doi.org/10.1046/j.0953-816x.2001.01717.x>
- Troncoso, X. G., McCamy, M. B., Jazi, A. N., Cui, J., Otero-Millan, J., Macknik, S. L., ... Martinez-Conde, S. (2015). V1 neurons respond differently to object motion versus motion from eye movements. *Nature Communications*, 6, 8114. <http://doi.org/10.1038/ncomms9114>
- Turatto, M., Valsecchi, M., Tamè, L., & Betta, E. (2007). Microsaccades distinguish between global and local visual processing: *NeuroReport*, 18(10), 1015–1018. <http://doi.org/10.1097/WNR.0b013e32815b615b>
- VanRullen, R. (2007). The power of the feed-forward sweep. *Advances in Cognitive Psychology*, 3(1), 167–176. <http://doi.org/10.2478/v10053-008-0022-3>
- VanRullen, R., & Thorpe, S. J. (2001). The Time Course of Visual Processing: From Early Perception to Decision-Making. *Journal of Cognitive Neuroscience*, 13(4), 454–461. <http://doi.org/10.1162/08989290152001880>
- Wickham, H. (2009). *ggplot2: Elegant Graphics for Data Analysis*. New York: Springer-Verlag.
- Yuval-Greenberg, S., Tomer, O., Keren, A. S., Nelken, I., & Deouell, L. Y. (2008). Transient Induced Gamma-Band Response in EEG as a Manifestation of Miniature Saccades. *Neuron*, 58(3), 429–441. <http://doi.org/10.1016/j.neuron.2008.03.027>